INT. J. REMOTE SENSING, 2002, VOL. 23, NO. 23, 5123–5128

Taylor & Francis
Taylor & Francis Group

Reflectance, dielectric constant and chemical content of selected sedimentary rocks

Q. J. TIAN†, P. GONG†‡, B. XU‡, X. WANG§, H. GUO§ and Q. TONG§

†International Institute for Earth System Science, Nanjing University, P.R. China, 210093
‡Center for Assessment and Monitoring of Forest and Environmental Resources, University of California, Berkeley, CA 94720-3110
§Institute of Remote Sensing Applications, Chinese Academy of Sciences, Beijing, P.R. China

(*Received 9 November 2000; in final form 5 May 2002*)

Abstract. Relationships among average spectral reflectance measured in the visible and near infrared (VNIR) region (0.4–2.5 μm), dielectric constant measured in the microwave region (0.5–18 GHz) and chemical content of 34 sedimentary rock samples were measured. The natural logarithm of the average spectral reflectance and that of the imaginary part of the dielectric constant were negatively correlated ($\rho = -0.60$). The average spectral reflectance correlated negatively with Fe_2O_3 ($\rho = -0.61$), Al_2O_3 ($\rho = -0.63$), K_2O ($\rho = -0.60$), TiO_2 ($\rho = -0.64$), and P_2O_5 ($\rho = -0.60$). The average imaginary part of the dielectric constant correlated positively with Fe_2O_3 ($\rho = 0.76$), K_2O ($\rho = 0.62$), and TiO_2 ($\rho = 0.70$). The average real part of the dielectric constant is highly correlated with the weight loss of the rocks due to burning (burnt loss) ($\rho = 0.92$), SiO_2 ($\rho = -0.96$), and CaO ($\rho = 0.91$).

1. Introduction

Optical remote sensing and radar remote sensing utilize different physical properties of the same object. They are often used in combination through image fusion for geological applications (Mather *et al.* 1998) and land-cover mapping (Solberg *et al.* 1994). The Fresnel equation suggests a relationship between the reflectivity and dielectric constant of an object in the same wavelength (Hapke 1993). The diurnal change of trees in a walnut plantation site was examined in the microwave and optical bands, with the microwave sensors taking measurements from inside the tree stems and optical sensors taking measurements from tree canopies (Way *et al.* 1991). However, there is no research reporting on the relationship between spectral reflectance in the VNIR region (0.4–2.5 μm) and the dielectric constant of the same object in the microwave region (0.5–18 GHz). This letter reports some preliminary results on the relationships among spectral reflectance, dielectric constant measured from selected sedimentary rock samples and rock chemical contents.

International Journal of Remote Sensing
ISSN 0143-1161 print/ISSN 1366-5901 online © 2002 Taylor & Francis Ltd
http://www.tandf.co.uk/journals
DOI: 10.1080/01431160210153976

Table 1. Albedo (R), averages of real (ε') and imaginary (ε'') parts of dielectric constants, and chemical contents in percentage of our experimental rock samples.

Sample	R	ε'	ε''	Burnt Loss	SiO_2	Fe_2O_3	Al_2O_3	CaO	MgO	K_2O	Na_2O	TiO_2	MnO	P_2O_5
Light grey limestone	35.67	8.498	0.348	37.35	6.12	0.64	1.32	53.29	0.73	0.34	0.05	0.08	0.04	0.08
Dark grey limestone	29.69	8.390	0.353	34.99	13.62	1.09	3.58	44.19	0.97	0.89	0.34	0.13	0.13	0.12
Black shale	10.22	5.984	0.441	16.41	54.63	2.46	7.44	13.40	1.44	2.39	0.43	0.36	0.02	0.61
Dark green mudstone	11.07	6.943	0.574	20.32	44.91	4.14	7.30	18.12	1.90	1.84	0.38	0.58	0.11	0.33
Black mudstone	15.13	6.897	0.625	18.79	47.07	4.13	7.52	17.30	1.93	1.85	0.38	0.61	0.11	0.27
Dark grey sandstone	20.22	5.456	0.358	3.59	75.82	4.20	9.05	1.65	1.49	1.93	1.07	0.36	0.12	0.23
Dark grey packsand	17.04	5.332	0.367	3.50	75.13	5.11	10.27	0.48	1.50	2.14	1.11	0.37	0.07	0.31
Grey green sandstone	24.69	5.562	0.480	2.44	76.50	3.51	11.24	0.37	1.23	2.63	1.32	0.48	0.04	0.23
Purple quartz sandstone	22.42	5.113	0.245	6.06	75.88	1.87	6.03	5.80	0.86	1.30	0.84	0.28	0.27	0.56
Grey quartz sandstone	41.10	4.702	0.277	1.28	94.20	0.99	1.29	1.09	0.28	0.30	0.19	0.06	0.03	0.16
Grey green siltstone	17.43	5.701	0.414	5.03	71.59	2.80	10.91	3.59	1.68	1.88	1.83	0.49	0.11	0.29
Purple siltstone	22.02	6.930	0.564	5.39	66.47	4.25	12.72	3.42	2.26	2.13	1.85	0.58	0.10	0.30
Purple sandstone	23.45	5.138	0.362	4.09	81.03	1.73	6.49	2.08	1.26	1.11	1.50	0.32	0.04	0.20
Grey limestone	22.59	5.904	0.556	5.64	75.06	2.76	7.51	3.81	1.31	1.93	1.00	0.36	0.04	0.22
Grey green sandstone	45.73	7.824	0.518	29.39	29.60	1.56	4.27	32.59	1.10	1.05	0.44	0.13	0.36	0.15
Incarnadine gritstone	12.17	7.577	1.041	19.28	34.66	11.73	7.85	19.91	2.85	0.76	0.89	1.41	0.42	0.49
Grey green sandstone	21.10	5.356	0.440	1.55	75.04	3.16	12.85	0.69	0.47	2.46	3.78	0.41	0.04	0.19

Table 1. (*Continued*).

Sample	R	ε'	ε''	Burnt Loss	SiO_2	Fe_2O_3	Al_2O_3	CaO	MgO	K_2O	Na_2O	TiO_2	MnO	P_2O_5
Black mudstone	14.40	8.279	0.278	41.13	5.25	0.19	0.53	52.03	0.34	0.12	0.06	0.01	0.02	0.08
Purple sandstone	8.86	6.869	1.245	2.95	68.78	5.95	13.39	0.98	1.01	4.52	1.74	0.64	0.05	0.22
Pale limestone	27.42	5.322	0.420	7.22	78.63	1.66	3.49	5.11	2.02	1.29	0.33	0.29	0.10	0.24
Pale limestone	36.95	8.605	0.320	42.07	2.77	0.36	0.63	52.50	1.28	0.11	0.06	0.02	0.02	0.08
Dark grey limestone	57.85	8.545	0.302	42.55	1.31	0.12	0.42	54.91	0.30	0.08	0.01	0.01	0.00	0.08
Purple siltstone	15.50	7.905	0.317	41.20	5.60	0.21	0.56	50.96	1.12	0.14	0.11	0.02	0.01	0.07
Pale gritstone	13.73	6.920	0.674	16.17	49.23	2.83	8.57	17.04	2.10	1.33	1.59	0.41	0.18	0.20
Purple mudstone	29.22	5.615	0.426	12.49	64.12	1.82	5.58	12.30	1.17	0.83	1.25	0.29	0.06	0.17
Brown sandstone	17.22	6.512	0.579	8.93	57.67	5.22	13.63	6.87	2.48	2.57	1.47	0.62	0.17	0.31
Caesious limestone	18.24	5.283	0.356	2.88	79.55	2.47	8.40	2.11	1.11	0.91	1.75	0.48	0.08	0.31
Pale grey dolostone	37.51	8.474	0.251	41.19	2.56	0.12	0.59	54.71	0.33	0.16	0.06	0.01	0.00	0.05
Caesious dolostone	43.37	5.420	0.281	1.32	95.25	0.30	1.22	1.11	0.21	0.09	0.19	0.06	0.03	0.03
Dark green sandstone	32.06	7.906	0.350	44.68	3.25	0.16	0.43	31.58	19.97	0.15	0.05	0.01	0.01	0.09
Grey black siltstone	17.94	5.745	0.369	4.82	74.53	3.32	8.64	3.47	1.09	2.05	1.16	0.40	0.55	0.27
Black mudstone	18.11	7.830	0.439	27.67	26.75	5.16	5.64	29.42	1.99	0.89	0.34	0.94	0.26	0.26
Grey Marl	10.24	6.521	0.558	12.10	54.49	5.34	10.18	10.31	2.74	2.39	0.95	0.91	0.19	0.34
Unnamed	26.21	8.546	0.292	37.23	11.95	1.20	2.01	45.24	1.01	0.48	0.24	0.23	0.10	0.18

2. Experimental methods

Thirty-four sedimentary rock samples of different type were collected in Xinjiang, China (table 1) and cut into slices, each with dimensions approximately 5 cm × 5 cm × 2 cm. One side of the samples was polished to allow dielectric constant measurements; the other side was kept fresh for spectral reflectance measurement. Dielectric constants of the rock samples were measured in the microwave region, between 0.5 and 18 GHz, using a dielectric probe system in the L, S, C, X and Ku bands (Ulaby *et al.* 1990). The probe tip of the instrument was placed on the polished section of the rock samples. The root mean squared error of measurement for the real part of the dielectric constant was less than 0.05, and less than 0.1 for the imaginary part.

The spectral reflectance of the rock samples was measured in the VNIR region (0.4–2.5 μm) using a portable spectrometer, GER MARK-V. Reflectance was measured by placing the spectrometer probe towards the fresh section of the samples in the laboratory under halogen lighting sources. The spectral resolution was 2–4 nm. Each sample was measured three times, and an average taken. The root mean squared error of measurement was less than 0.03. For each rock sample, the average real part of the dielectric constant, ε', the average imaginary part of dielectric constant, ε'', and the average spectral reflectance, R, were calculated. At the same time, chemical analyses of all rock samples were made, and the SiO_2, Fe_2O_3, Al_2O_3, CaO, MgO, K_2O, Na_2O, TiO_2, MnO and P_2O_5 content and their proportions of weight loss due to burning (burnt loss) were measured. The averages of sample reflectance, dielectric constants and percentage chemical contents are shown in table 1.

3. Data analysis

Table 2 shows the correlations among R, ε', ε'', and the chemical contents of selected rock samples. It can be seen from table 2 that the magnitudes of many correlations are greater than 0.6. In particular, the average reflectance is inversely correlated with Fe_2O_3 ($\rho = -0.61$), Al_2O_3 ($\rho = -0.63$), K_2O ($\rho = -0.60$), TiO_2 ($\rho = -0.64$), and P_2O_5 ($\rho = -0.60$), where ρ is the correlation coefficient. In contrast, the average imaginary part of the dielectric constant, ε'', has positive correlation with Fe_2O_3 ($\rho = 0.76$), K_2O ($\rho = 0.62$), and TiO_2 ($\rho = 0.70$). Interestingly, although neither are linearly correlated with R nor with ε'', the average real part of the dielectric constant, ε', complemented R and ε'' well due to its very significant correlation with the burnt loss of the rocks ($\rho = 0.92$), SiO_2 ($\rho = -0.96$), and CaO ($\rho = 0.91$). Among all the chemical contents, only MgO and MnO have low correlation with any of R, ε', and ε''. From the above analysis, it is concluded that R, ε', and ε'' of these sedimentary rock types are determined by their chemical constituents to some degree.

Scatterplots among R, ε', and ε'' and between each of R, ε', and ε'' with each chemical constituent were drawn up for exploratory analysis. The most interesting plot was between R and ε'', as shown on the left of figure 1. R is negatively correlated with ε'' ($\rho = -0.48$). However, the scatterplot between the natural logarithm of R ($\ln R$) and the natural logarithm of ε'' ($\ln \varepsilon''$) revealed a larger correlation coefficient ($\rho = -0.60$), as shown on the right of figure 1. The least squares fit is $\ln \varepsilon'' = 0.59 - 0.47 \ln R$. This is a geometric relation between R and ε'' ($\varepsilon'' = e^{0.59} R^{-0.47}$). This relationship has two related implications that need further verification: (1) it may not be necessary to use both reflectance and SAR backscatter data to differentiate sedimentary rock types; and (2) the property may be a useful 'signature' in differentiating sedimentary rocks from non-sedimentary rocks or other surface cover types.

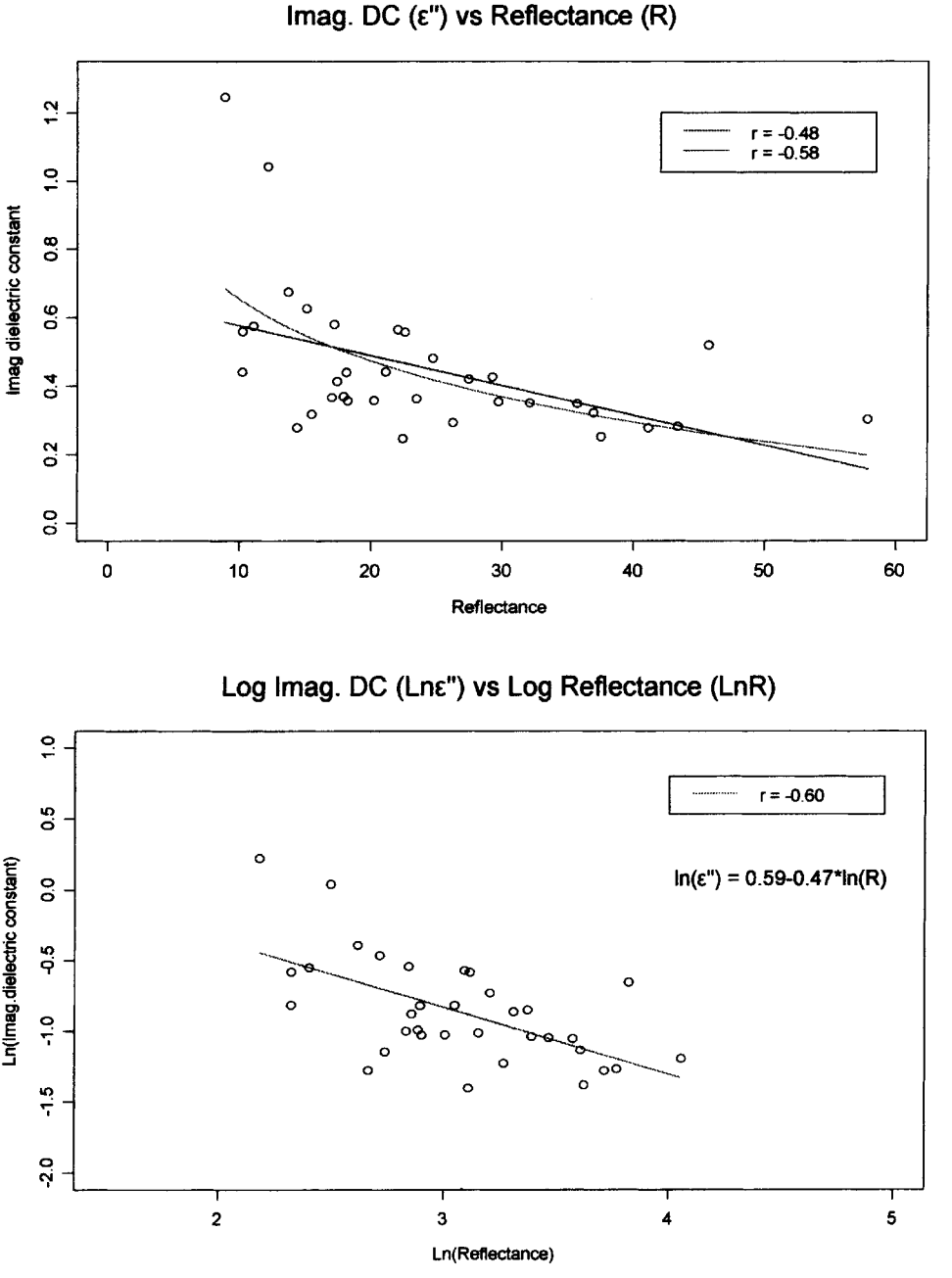

Figure 1. Relationship between albedo (R) and average imaginary part of the dielectric constant (ε') (upper), and that between ln R and ln ε'' (lower).

Some initial work was done to explore the relationships between narrower bands (corresponding to those of Landsat Thematic Mapper) of the reflectance measurements and the five separate microwave bands. Interestingly, they all exhibit negative correlation (-0.07 to -0.51).

Table 2. Correlations among R, ε', ε'' and rock chemical contents.

	R	ε'	ε''	Burnt Loss	SiO_2	Fe_2O_3	Al_2O_3	CaO	MgO	K_2O	Na_2O	TiO_2	MnO	P_2O_5
R	0.23	−0.48		0.34	−0.24	−0.61	−0.62	0.38	−0.01	−0.60	−0.40	−0.64	−0.22	−0.60
ε'		0.03		0.92	−0.96	−0.18	−0.50	0.91	0.15	−0.43	−0.52	−0.17	−0.04	−0.42
ε''				−0.26	0.14	0.76	0.57	−0.29	0.03	0.62	0.33	0.70	0.27	0.33

4. Discussion and conclusions

These results indicate that there exists a geometrical relationship between the average reflectance measured in the VNIR region and the average imaginary part of the dielectric constant measured in the microwave region for sedimentary rocks selected in this study. These results are interesting as no similar work has been reported. They may be useful for integrated use of microwave and optical remote sensing data for surface cover classification and ecological parameter estimation. For example, it might be difficult to unambiguously monitor canopy water status or soil moisture with optical sensors but they could be estimated from microwave backscatter, which is sensitive to variation of dielectric constant (Way *et al.* 1991, Bindlish and Barros 2000).

The explorative analysis of statistical correlation should be done in more detailed spectral ranges and be extended to other types of rocks and surface covers. Further research is also required to test the validity of these findings with remotely sensed data acquired from airborne and satellite borne platforms.

The percentage chemical contents for most constituents in the rocks selected in this study are strongly correlated with either R, ε', or ε''. If these relationships hold after additional tests, then some practical instrument may be built based on these strong correlations so that most chemical constituents in these rocks may be estimated to a specified level of accuracy.

Acknowledgment

This research was partially supported (P. Gong) by NSF of China (49825511).

References

Bindlish, R., and Barros, A. P., 2000, Multifrequency soil moisture inversion from SAR measurements with the use of IEM. *Remote Sensing Of Environment*, **71**(1), 67–88.

Hapke, B., 1993, *Theory of Reflectance and Emittance Spectroscopy* (New York: Cambridge University Press).

Mather, P. M., Tso, B., and Koch, M., 1998, An evaluation of Landsat TM spectral data and SAR-derived textural information for lithological discrimination in the Red Sea Hills, Sudan. *International Journal of Remote Sensing*, **19**, 587–604.

Solberg, A. H. S., Jain, A. K., and Taxt, T., 1994, Multisource classification of remotely sensed data—fusion of Landsat TM and SAR images. *IEEE Transactions on Geoscience and Remote Sensing*, **32**, 768–778.

Ulaby, F. T., Bengal, T. H., Dobson, M. C., East, J. R., Garvin, J. B., and Evans, D. L., 1990, Microwave dielectric properties of dry rocks. *IEEE Transactions on Geoscience and Remote Sensing*, **28**, 325–335.

Way, J. B., Paris, J., Dobson, M. C., McDonald, K., Ulaby, F. T., Weber, J. A., Ustin, S., Vanderbilt, V. C., and Kasischke, E. S., 1991, Diurnal change in trees as observed by optical and microwave sensors—the EOS synergism study. *IEEE Transactions on Geoscience And Remote Sensing*, **29**, 807–821.